

Volker Gollnick, Jannis Lührmann, Felician Danquah, Arno Semke, Thomas Müller, Jens Thöben

Institute of Air Transportation Systems, Hamburg University of Technology

Corresponding author: Prof. Dr.-Ing. Volker Gollnick, phone: +49 40 42878 4197, fax: +49 40 42878 2979, email: volker.gollnick@tuhh.de; https://orcid.org/0000-0001-7214-0828

Abstract

For the past few years the Lilium-Jet is fascinating the aviation community. On the one hand its esthetic configurational design approach attracts people, on the other the electric drive and energy storage raises discussions regarding its success. Since only very few technical information of this vehicle is available in the scientific public, the research question is about a better understanding of the design concept. This article presents the approach and results of an experimental study regarding the characteristics and behavior of the Electrical-Powered-Ducted-Thrust-Vectoring-Flap wing concept. Therefore, the first part provides an introduction of the Lilium-Jet based on publicly available information. The following section enrolls a methodology to answer the research question. Based on the description of the methodology some of the results of the wind tunnel tests are presented and discussed indicating, the installation of the ducted fan on the flap provides some significant advantages in the efficiency of the lift generation at different flight states.

Keywords: Lilium jet concept, Ducted Electric Thrust Vector, aerodynamics, characteristics, aircraft design

1. Introduction

The "Lilium Jet" first published in 2015, is a new approach for the upcoming "urban air mobility" air transportation concept, [1], [3]. Urban Air Mobility is understood as a concept to provide a new individual transport mode within large cities and metropolitan regions to overcome distances up to 300km within 1 hour. The vehicle concept itself comprises various new technology features like a battery based electric drive system and a distributed propulsion ducted electric thrust vectoring flap, which raise the interest in a deeper understanding. However, only very limited scientific literature and information is available for a detailed technical insight into the concept. The only one provided by Lilium itself is a White Paper published April 2021, which discusses the entire concept at a more generic level, [6].



figure 1: Artist impression of the Lilium Jet, [1]

This White Paper gives some official information about the overall concept of the distributed propulsion Ducted-Electric-Thrust-Vector (DETV). Although no exact figures are provided, some design points are given. The design mass baseline is the takeoff mass limit of 3175kg of the EASA special condition specification EASA-SC-VTOL-01, [4]. Based on this, a seven seater including pilot is defined with 700kg payload. A wing span of 13.90m and an overall length of 8m have been set as geometric dimensions.

There is no doubt, that for urban regional transport, which has been defined as the design mission for the jet, a relevant overall travel distance is a vital factor of success. 200 km target range and a cruise flight speed of about 300 km/h are defined for the generic concept, as declared in the White Paper.

Parameter	Value	Unit
Payload	700	[kg]
Range	200	[km
Take Off mass ¹	< 3175	[kg]
Cruise speed	300	[km/h]
Wing span	13.90	[m]
Overall length	8	[m]

table 1: Design figures of the 6 passengers plus pilot Lilium jet, [6]

With the actually available battery density of 275 Wh/kg, and a short term potential of 330 Wh/kg within the next 5 years, the intended performance as given in the White Paper may be hard to achieve at the intended entry into service 2025, [10]. However, there is a potential to achieve 400Wh/kg in 2030, [5], [8]. Actually, the envisaged performance data of the Lilium jet have been adapted and reduced to 250km/h and 175km range, [2].

Further technical information is partially given on the company's homepage and many public websites, [1], [6], [7], [9], [10]. A real comprehensive composition of the entire design is still missing, since there are various information and data publicly circulating.

Due to the challenge of limited energy density of today's batteries and the scarce information about the characteristics of the vehicle, there is an interest in a better understanding of some of the key features of the vehicle. Especially the efficiency of the aerodynamics characteristics in conjunction with the innovative propulsion concept is important, if only limited electric energy is available.

The definition of such a full electric vehicle concept with VTOL and cruise capabilities requires an efficient lift and cruise concept, as well as an efficient thrust vectoring concept.

According to Lilium about 60% of the entire lift is generated by the main wing, while 20% is provided by the canards and another 20% by the fuselage, [10]. The direct lift configuration with lifting canards chosen by Lilium is an appropriate part of the design solution, because instead of creating negative lift as on conventional aircraft, positive lift is generated for e.g. pitching up and climbing.

Further, the geometry of the main wing and canards published by Lilium shows a very short forward wing portion of the aerodynamic wing profile, while the DETV seems to be quite large. Typically, the forward part of a wing profile provides the major part of aerodynamic lift through the low pressure area at the upper wing.

If this area is quite small, as for the Lilium wing concept, the question is raised, how the efficient lift production is realized in this concept?

Today the configuration consists of in total 30 distributed DETV installed on the flaps, [2]. 18 DETV are located on the main wing, while 12 are placed on the canards resulting in a thrust capacity distribution of 60%:40% between main wing and canards.

This setup provides a good distributed thrust share between forward (canard) and backward (main wing) part of the vehicle, which allows for good pitch stability in hover through thrust vectoring control. However, this requires sophisticated flight control for good handling qualities.

Resuming the brief analysis of the Lilium jet concept the purpose of this study is directed to a better understanding of the lift creation in conjunction with the flap based ducted fans for propulsion and control. This is especially challenging, if only a very few real data of the configuration of interest is available.

2. Analysis of the wing and canards with ducted electric thrust vectors

Compared to other concepts, the installation of the ducted fans in the Lilium concept is located on the flaps for propulsion and control, rather than on the forward part of the wing, e.g. NASA N3-X, ONERA concept aircraft, [17], [18], [19].

This architecture allows the use of the DETV as tiltable thrust vectors, which is an efficiency feature of the concept, because the thrust direction can contribute to vertical flight during hover and transition, while it is directed to forward flight in cruise. A similar concept has been investigated by the University of Illinois and Rolling Hills Research Corp., [18], [22].

-

¹ Limit of EASA SC-VTOL-01

Compared to the studies of the University of Illinois in our case valid initial geometric data are not yet available, which requires additional investigative effort.

2.1 Methodology

The entire methodology is based on four pillars, which at first collects and generates necessary geometrical data.

In a second step a post projection of the Lilium concept jet is performed using handbook methods and the generated geometric data.

The third step addresses the development of a scaled wind tunnel model to investigate the principle aerodynamic behavior of the concept.

At last, the fourth step comprises a wind tunnel test campaign to investigate some aerodynamic characteristics of interest.

2.1.1 Geometric data generation

The greatest challenge for the research in this case is the acquisition of realistic basic geometric data. Since only a very few are given in public literature the first task is the estimation of geometric data for the fuselage and wing geometry.

For the vehicle, Lilium gives the following main sizes as shown in figure 2.



figure 2: Main sizes of the Lilium concept, [1], [7]

More required geometric data could be generated through measuring from available pictures and sketches, which may have distortions. Therefore, these distortions have to be identified, which was done using the public domain tool ImageJ, [23].

Taking the wing span and the fuselage length as the reference, scaling and distortion factors can be identified for each direction from the pictures referred to the left in figure 3, as listed in table 2.

Original	Scaling factor M_i	Scaling factor M _j
Top view	$M_x = 78.7 \frac{Pixel}{Meter}$	$M_y = 87.9 \frac{Pixel}{Meter}$
Side view	$M_y = 143.25 \frac{Pixel}{Meter}$	$M_z = 146.25 \frac{Pixel}{Meter}$

table 2: Derived scaling factors of the sketches

The results presented in table 2 are only an example of our individual analysis case, which shall show a part of the methodology and typical results.

It turns out, that the length of the sketch in top view has to be shortened by 10% (78.7/87.9=0.89533) to achieve correct proportions.

$$M_{scaled} = \frac{M_i}{M_i} \tag{1}$$





figure 3: Corrected proportions (right image) of the Lilium Jet sketch, derived from [1]

As shown in figure 3 the distortion in the original sketch at the left becomes obvious as compared to the right corrected sketch, which is slightly smaller. Since the measured distortion of 10% in each direction is quite small, the differences in the pictures are also small.

With these corrected geometry data, a post projection of the vehicle was performed.

Before, the wing, fuselage and canard geometry have to be estimated, the profile characteristics must be described.

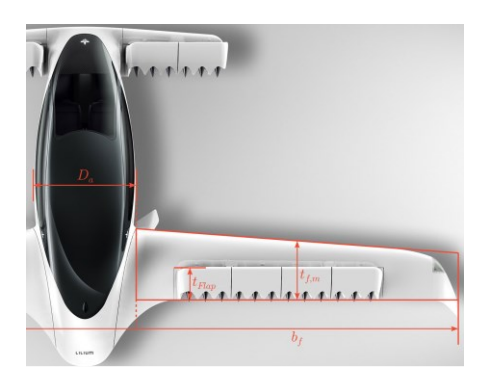


figure 4: Estimated wing chord length and ducted fan length

The profile of the wing was derived from a sketch of the Lilium website, [1], [16]. The Lilium feasibility study describes a relative profile thickness of 0.12, [7]. Further, using the sketch scaling at the given flap chord length t_f =700mm (duct length), the overall chord length of the main wing can be estimated as t_w =1300mm approximately.

Assuming a simplified tapered wing area and subtracting the contribution of the fuselage because of its own lift and drag characteristics the main wing area can be determined as

$$S_w = (13.9m - 1.7m) \cdot 1.3m = 15.86m^2$$
 (2)

Taking the fan diameter of 295mm and its duct length t_f of 700mm, as stated by Lilium, the webpage drawing was tuned, so that the fan diameter and the duct length fulfil in a scaled way the proportion of the fan diameter. This drawing size was taken as a baseline to determine the maximum profile thickness and its distance to the nose to approximately d_p =130mm and x_d =330mm, where any curvature was neglected.

Comparing the drawing to various NACA profiles with a relative thickness of 0.12 as shown in figure 5, it turned out, that a NACA 4412 profile seems to provide a relatively good fit.



figure 5: Approximation of the wing profile selecting NACA 4412 profile, [16]

figure 5 shows, that especially for the forward part of the wing the tendon curvature fits better for the NACA 4412 profile.

However, in both cases there is a deviation of the wing profile along the DETV of approximately 200mm, compared to the geometric estimation. The discrepancy compared to the graphical estimation results from the extended length of the ducted fan.

Because this section does not affect the aerodynamic performance of the forward wing profile, this discrepancy is accepted. For the overall wing analysis, an overall chord length of t_f =1300mm was chosen. With this, a maximum thickness at 30% of the chord length was estimated, which is about 390mm from the nose, taking the chord length of t_f =1300mm.



figure 6: Approximation of the hinge position

From the scaled drawing in figure 7, a relation of

$$\frac{x_{hinge}}{t_f} \approx \frac{4}{5} \tag{3}$$

was estimated, which is compliant to the geometry at DETV 5 counted from the outside of the wing as shown in figure 6. DETV 5 should be also representative for the flow analysis of the active DETV during the wind tunnel tests.

The hinge position x_h was determined as 590mm roughly also by visual comparison.

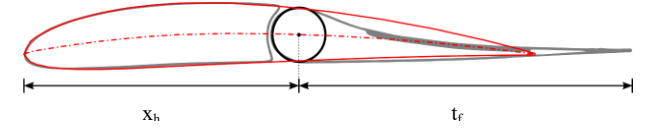


figure 7: Hinge position estimation, [16]

In a very similar way, data for the fuselage, the canards and the landing gear were created. Here, the fuselage was approximated as a NACA 2725 with a 10% backwards shifted maximum thickness of 21% instead of 25%.

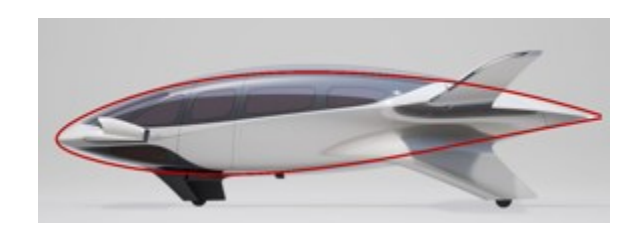


figure 8: NACA 2725 approximated fuselage shape profile

The landing gear was approximated by a NACA 0560, while the canards were scaled like the main wing. At the end of this analysis process the following figures for the wetted areas have been estimated, which are relevant for the drag estimation.

Component	Wetted surface S_{wet} [m^2]
Main wing	28.65
Canard	9.13
Fuselage	33.75
Landing gear front	0.74
Main landing gear	6.36

table 3: Estimation of the wetted areas of the vehicle main components

Looking at the figures, the wetted area of the main landing gear may turn out as too high, compared to the other figures, as further drag estimations have shown. Therefore, for a subsequent iteration a more slender profile will be selected.

At the end of the graphic analysis and also considering e.g. a main wing span extension by winglets, the following key data have been calculated using handbook methods, e.g. provided by Raymer, [20], [21].

Attribute	Value
Wing span b_{Lilium}	13.8m
Overall length l_{Lilium}	8m
Main wing area S_{Ref} w/o. fuselage	15.66m²
Wing area Canard S_{Canard} w/o. fuselage	5.54m ²

table 4: Approximated main geometric sizes of the Lilium concept aircraft

For such a canard wing area, with a given canard wing span of 6.3m the resulting canard wing chord will be around 0.8m. A lot of more detailed data have been elaborated in [20].

There is no doubt, that the chosen approach is a pragmatic engineering method, which includes some sources of inaccuracies. Reading and measurement errors have to be recognized as well as errors in the approximations. The use of handbook methods add inaccuracies too. However, for the purpose of creating a first public data basis about this fascinating concept, the chosen approach is assumed to be acceptable.

2.1.2 Post projection of the Lilium jet concept

In a second step during a post projection process, based on the well-known Raymer handbook methods, also first performance data could be achieved, [21].

At first the XFOIL-tool was used to determine the main characteristics of the NACA 4412 wing profile, which led to lift curves as shown in figure 9 for cruise condition at 3000m and 300km/h cruise speed, [24]. Although has adopted these figures to lower values, the study still uses the data of the generic concept to keep consistency, [7].

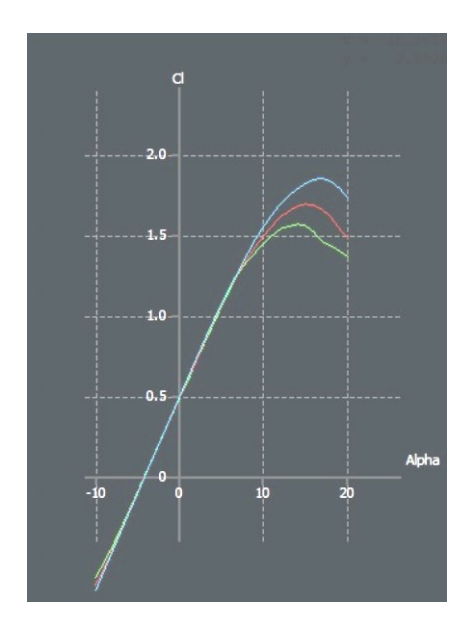


figure 9: NACA 4412 calculated lift curves based on the measured geometry for different Reynolds numbers (10⁶ in green, 2·10⁶ in red, 5·10⁶ in blue)

The calculations do not show significant differences in the gradient, so the resulting gradient was chosen. The resulting lift characteristics are summarized as

NACA 4412 profile characteristics				
Lift gradient $C_{l\alpha}$	5.97			
Zero lift angle $lpha_0$	-4.8°			
Zero lift coefficient C_l	0.5			
Zero pitch coefficient C_{m_0}	-0.1064			

table 5: Lift characteristics of the NACA 4412 wing profile

The overall lift curve has been determined according to figure 10.

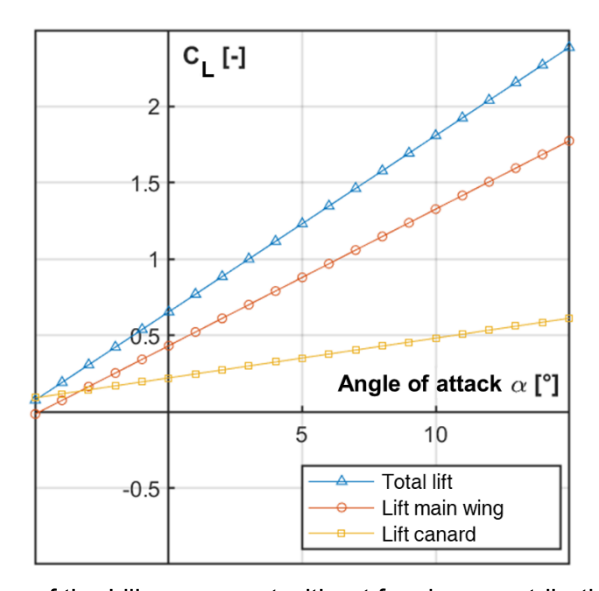


figure 10: Overall lift curve of the Lilium concept without fuselage contribution of approximately 20%

Assuming an angle of attack in cruise of 0° and installation angles for the canards of 3.67° and 0° for the main wing and canard a cruise lift coefficient of C_L = 0.62 can be achieved at α =0°. This does not include any contribution of the fuselage. If according to Lilium a 20% lift contribution will be assumed,

the conceptual calculation will lead roughly to C_L = 0.81 in cruise, which is far above the calculated required design lift coefficient of C_{Ldesign} = 0.62.

$$C_{L,design} = \frac{2 \cdot m_{MTOM} \cdot g}{\rho \cdot S_{Ref} \cdot v_{cruise}^2} = 0.62$$
 (4)

which is calculated for 3000m cruise altitude and 3175kg m_{TOM}, at 300km/h cruise speed.

Estimating the drag of the configuration, while neglecting any wave drag, a zero drag coefficient of CD0 = 0.06525 would be achieved, if all calculated wetted areas are taken into account.

Part	$C_{D0}[-]$	k_{CD_i}
Main wing	0.00625	0.051
Canard	0.00208	0.055
Fuselage	0.00829	0
Main landing gear (too high)	0.04562	0
Forward landing gear	0.00302	0
Overall concept	0.06525	0.0256

table 6: Zero drag estimation of the overall concept, [20]

Based on the wetted areas as shown in table 3 and the consideration of surface roughnesses a significant value is achieved driven by the drag of the main landing gear, which might be oversized due to the chosen thickness of the profile of the landing gear cowling. If the entire landing gear contribution is neglected an overall zero drag C_{D0} = 0.01662 will occur, which is considered to be more realistic. The total drag C_D can be calculated with

$$C_D = C_{D0} + k_{CDi} * C_L^2 (5)$$

 $C_D=C_{D0}+k_{CDi}*C_L^2 \eqno(5)$ to a value of C_D = 0.075 for the cruise configuration including landing gear drag. However, taking the calculated design lift coefficient of the wing and the canards of C_{Ldesign} = 0.62 into account, an overall lift to drag ratio of

$$E = \frac{c_L}{c_R} = 8.27 \tag{6}$$

 $E=\frac{c_L}{c_D}=8.27 \tag{6}$ could be estimated. In these calculations additional flow effects of the sucking DETV are not yet included which may increase the upper surface flow speed and the low pressure distribution. As a result, the L/D efficiency including the suction speed of the DETV is expected to be much higher. This topic will be focus of further research.

2.1.3 Wind tunnel test model design

It is not the intention to identify the exact figures, which are property of the company, but it is intended to get a better understanding of the principle physical characteristics of the wing, especially regarding the aerodynamic – propulsion interaction.

The wind tunnel model, intended to be used for the aerodynamic analysis, was designed according to simplicity, flexibility and cost.

The ducted fan of the DETV is represented by a model impeller. This approach was chosen because of cost reasons of available items. The diameter of the impeller is driving the scale of the model, which is set to 1:3.3 due to 295mm original diameter of the Lilium thrust vector and 90mm diameter of the chosen model impeller. Following this scale the geometry of the test model is defined as given in figure 11.

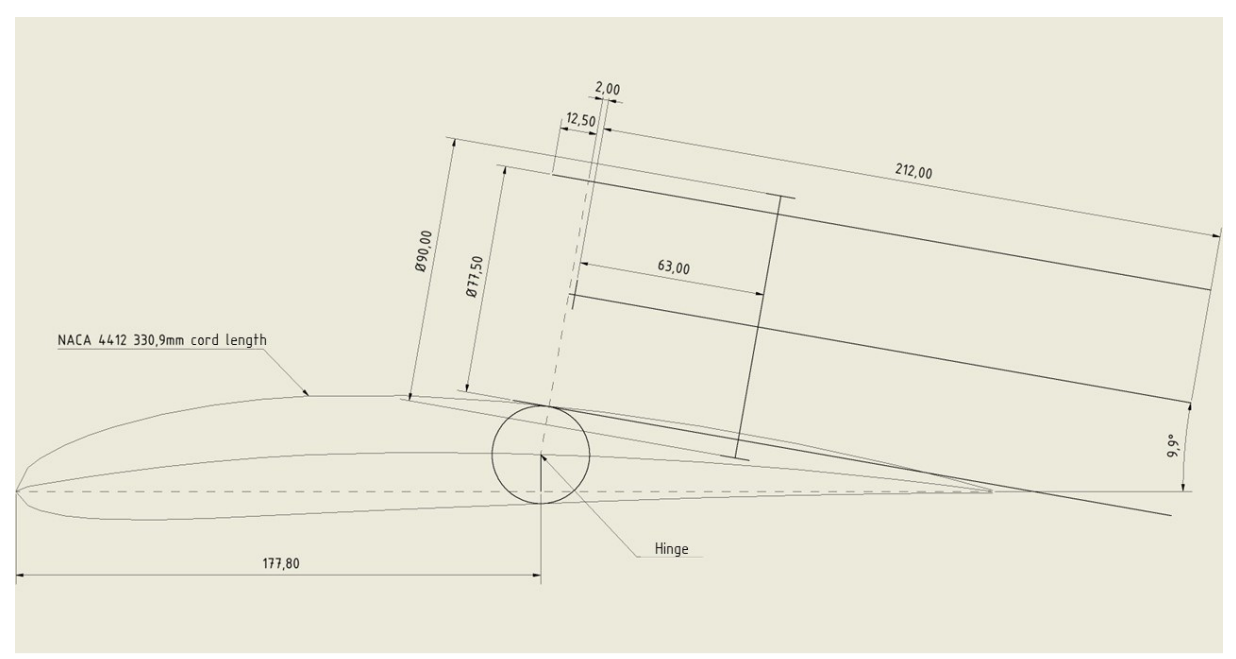
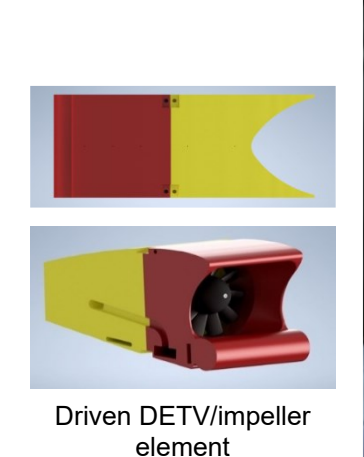


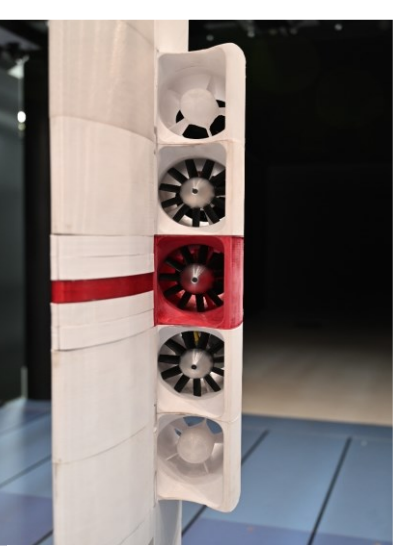
figure 11: Sizing of the wind tunnel wing model

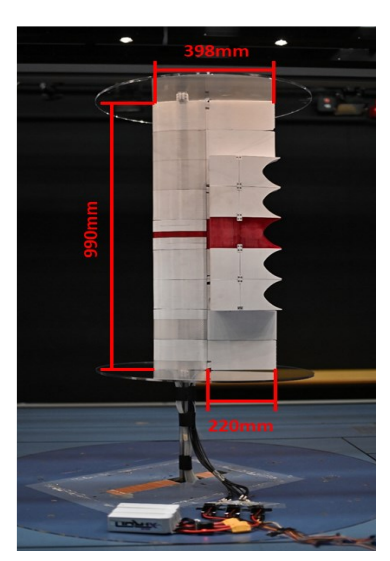
Following this method, it was possible to approximate the wing profile by a NACA 4412 profile with a chord length of 330 mm for the model. Applying the scale factor of 1:3.3 figure 4 provides the model parameter.

The hinge position of the flap was determined to 177.8 mm as shown in figure 11. Based on this geometrical analysis, the wind tunnel model was created.

The entire model was built of 5 modular DETV segments, where the outer two were built as dummies only to represent a broader part of the upper airfoil section of the DETV. In the middle colored in red a driven DETV and a forward wing foil are installed, which are fully equipped with 24 pressure holes. As visible in the picture in the middle of figure 12 the modular concept, which allows a variable reconfiguration also for the canard causes some inaccuracies in the connection of the elements, resulting also in inaccurate measurements.







Front view of the wing installation

Top view of the wing installation

figure 12: Driven DETV test model and test wing setup

All components have been produced using 3D printing technologies, which especially allows for a quite simple integration of the pressure holes of 0.8 mm. For the later performance of a full measurement campaign the red-colored front section, equipped with the pressure holes can be placed at different positions in front of the full active impeller, which allows the investigation of various flow conditions.

Since a key aspect of the research is directed to the lift behavior at the leading edge of the wing and the transition between clean wing and DETV, 24 pressure probes a placed as shown in figure 13.

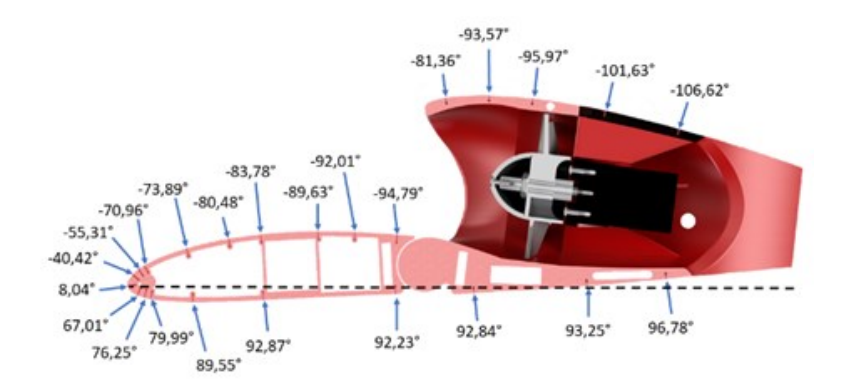


figure 13: Pressure probe distribution on the wing test section

Knowing about the simplicity and cost effectiveness of this chosen model approach, the subsequent investigations are fully understood as principle qualitative results, indicating the benefital effects of the concept.

2.1.4 Wind tunnel tests

At fourth, wind tunnel tests have been performed to describe the interaction between the airfoil and the DETV to analyze the aerodynamic lift characteristics and cross coupling with the propulsion. The Hamburg University of Technology operates a wind tunnel containing 3m wide and 2m high open

The Hamburg University of Technology operates a wind tunnel containing 3m wide and 2m high oper test section. The length of the test section is about 5.5m.

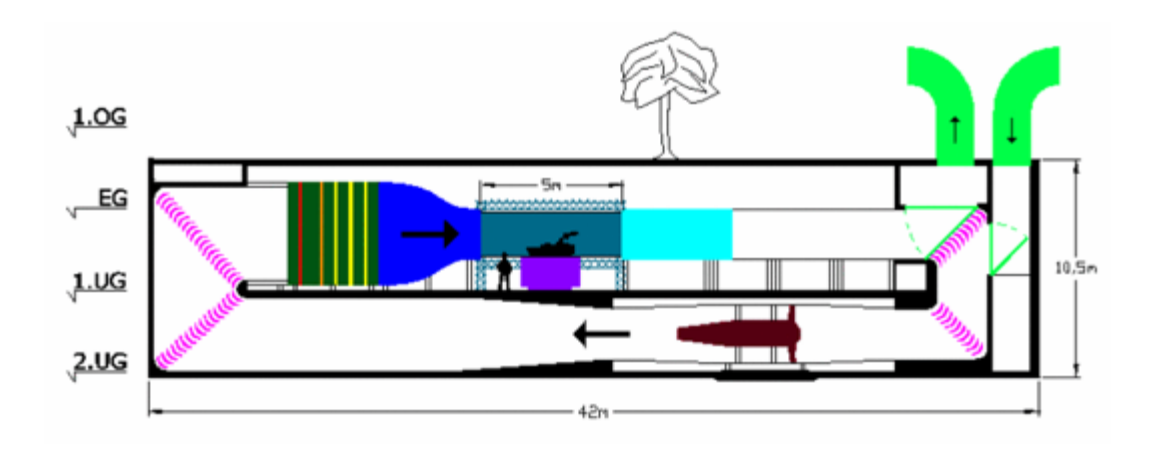


figure 14: Overview about the TUHH wind tunnel

The test section has a 6m² cross section and the maximum flow speed is 35 m/s. Due to that limitation adequate Reynolds conditions could not be fulfilled, since the Re-number for the cruise condition of the full scale Lilium concept aircraft would be:

$$Re = \frac{v \cdot l}{v} = \frac{83.3 \frac{m}{s} \cdot 1.22 \, m}{1.863 \cdot 10^{-5} \frac{m^2}{s}} = 5.45 \cdot 10^6 \tag{7}$$

A fulfillment of the Reynolds-requirement was not possible, because of the limited availability of impeller diameter, wind tunnel size and temperature control.

However, for a principle investigation of the characteristics, the wind tunnel would provide Re-numbers up to 2.29*10⁵ only, which correspond to low speed flight conditions of the Lilium jet. These flight conditions are typical for hover to cruise transition, which on the other hand are of particular interest, because here the different tilt angles of the DETV-flap occur with relevance.

Looking at the flight state analysis of the scaled Lilium concept jet as shown in table 7, flight speeds up to 180 km/h (50m/s) could be observed, but also low speed ranges of 0 - 50km/h (13.88m/s).

The wind tunnel test conditions were derived from video analysis of Lilium flight test publications, [1]. During the visual analysis the following test points have been identified.

Flight phase	Flap elevation angle [°]		Flight Speed [km/h]	Clip [min:s]	
	Main Wing	Canard			
Vertical Takeoff	90 - 80	90 - 80	0 - 50	0:00 0:13	
Departure	80 - 0	80 - 0	50 - 150	0:13 1:05	
Accelerate to 180 km	0	010	150 - 180	1:05 1:20	
Steep Climb	010	05	180	1:20 1:29	
Full Transition	0	0	180	1:29 1:40	
Angle of Bank	0 30	60 170	170	1:40 2:15	
Shallow Descent	0 20	0 40	<i>170</i> → <i>150</i>	2:20 2:35	
Steep Descent Approach	2090	4090	150 → 50	2:35 - 4:14	
Landing	90	90	50 → 0	4:14 - 4:30	

table 7: Flight state analysis of Lilium flight test

The analysis of the various sequences of the video clip also provides some indications of the flap tilt angles for the main wing as for the canards. These were also used for the definition of the various test cases.

Based on these flight test conditions a wind tunnel test matrix was established as shown as an extraction in table 8.

	Air speed	Flap angle	Thrust level	Ducted fan installed (Yes/No)	Angle of attack	Flight phase	Target
1. Configuration	30 m/s	0°	0%	Yes	0°	N/A	Reference
2. Configuration	30 m/s	0°	50%	Yes	0°	Cruise	Calibration
3. Configuration	30 m/s	0°	75%	Yes	0°	Cruise	Calibration
4. Configuration	30 m/s	0°	100%	Yes	0°	Cruise	Calibration
5. Configuration	28 m/s	0°	Dependent on previous tests	Yes	0°	Cruise	Proof of lift

table 8: Exemplary extract of the wind tunnel test matrix, [16]

Using these test conditions overall 37 trials have been performed at flow speeds up to 30 m/s, with a thrust setting of 0 and 100%. The measurements were performed for 5 seconds with a sampling rate of 10 Hz.

First promising results drove an increase of the thrust setting up 100%. The incoming flow speed was stepwise increased in 2 m/s increments.

2.2 Discussion of the results

In the following, some of the major results of the entire test campaign are presented and discussed. To validate the pressure measurements these were compared to force measurements of the calibrated 6-component wind tunnel load cell.

At first the lift coefficient was investigated by wind tunnel measurements, which at least confirm a very similar slope as calculated in figure 9 by XFOIL. It must be mentioned, that this similarity occurs only,

if the thrust is set to 45%, while at idle the lift curve is located at lower values and shows a lower gradient. All measurements have been performed at 15m/s flow speed.

figure 15 shows a quite good correlation of both measurements over a wide range of angle of attack, which gives confidence in the pressure measurement setup. Based on this verification and validation results further measurements have been performed.

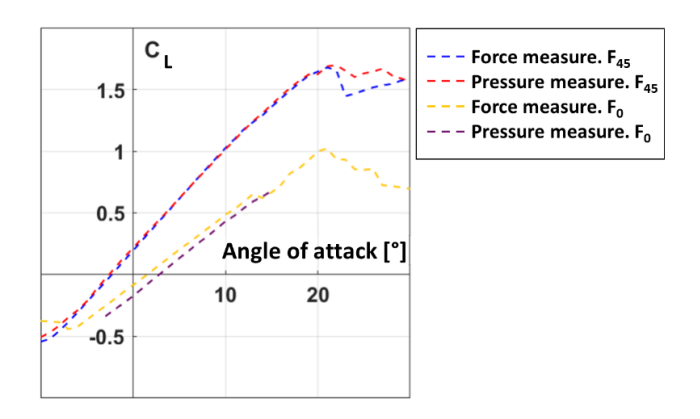


figure 15: Lift coefficient depending on angle of attack for force and pressure measurements

In a further step, various flap angles were investigated at different flow speed (V-x in m/s), as shown in figure 16. At a flap setting of 0° (lower curves) the lift coefficient shows a quite flat behavior at different thrust settings and varying flow speeds. The lower the flow speed the higher the lift coefficient, which indicates, that blocking by the DETV dummy ducts becomes an issue at higher flow speeds. This also reduces the gradient of the curve. On the other hand, tilting the flap to 20° or 40° increases the lift coefficient significantly (upper curves).

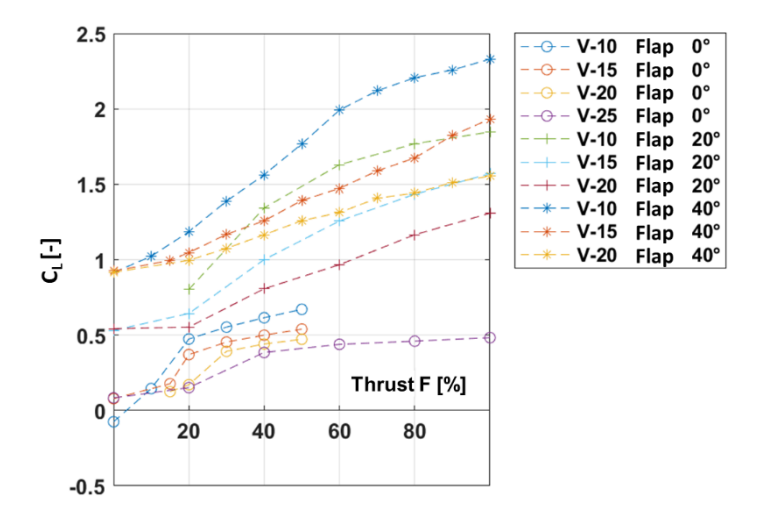


figure 16: Lift coefficient depending on flap angle and thrust setting

This effect becomes of major relevance during transition from hover to forward flight. Tilting the flap towards 40° and increasing the thrust level from 0% to 100% at low flow speed condition of v=10m/s result in a significant increase of the lift coefficient:

$$C_{L40^{\circ}}(F = 100\%) = 2.3$$

In this measurement the component of the thrust of the DETV in lift direction at a tilt angle of 40° was not considered. So, without any suction effects of the DETV the lift coefficient occurs much lower:

$$C_{L40^{\circ}} (F = 0\%) = 0.91$$

The lift coefficient occurs about 2.5 times higher at 100% thrust setting, which shows the significant positive aerodynamic-propulsive coupling effect of the DETV flap concept of the Lilium jet concept. Interestingly, the L/D ratio as the efficiency indicator shows at C_L =0.91 an increase of roughly 38.5%

higher compared to the calculated design L/D ratio at C_L =0.62 for this experimental principle test model, which hints to a minor impact on the drag increase of the 40° flap angle. It is

$$\frac{C_{L40^{\circ},100\%}}{C_D} = \frac{2.3}{0.2007} = 11.46 \tag{8}$$

The applicability of this increase in cruise configuration is to be considered carefully and must be verified in full scale but it indicates the approximate improvement due to this concept.

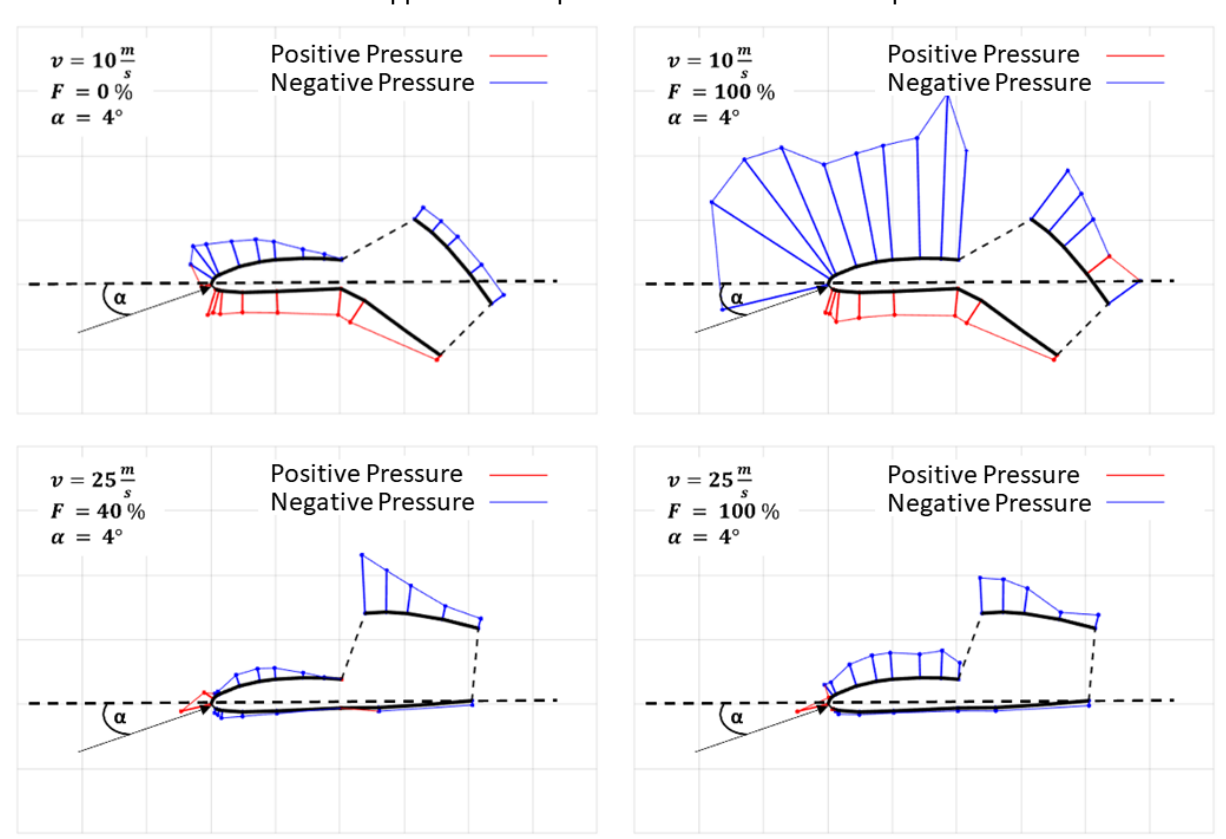


figure 17: Pressure distributions of the DETV at different flap and thrust settings

At last, at the top of figure 17, at low flow speeds (10 m/s) the DETV thrust increases the pressure distribution significantly, especially if the flap deflection is high (40°) as shown in the pictures top left and right. The suction effect of the fan seems to be quite high and inducing also lift generation on top of the fan. This effect is assumed to be one of the major benefits of the concepts

Further, also in forward flight at 25m/s (bottom left and right) the DETV increases the pressure distribution at high thrust levels. Looking at the forward flight condition shown at the bottom right, the DETV increases and improves the aerodynamic performance of the forward part of the wing although it is relatively short.

As a conclusion the impact of the DETV at the hover, low speed condition as well as at the forward flight condition is in all cases beneficial, as long as the certain thrust level is given. A certain thrust level is required for controlling the vehicle. The high pressure portion, typically below the profile is very much reduced to the nose area and some low pressure areas are also observed below the profile.

During the tests it was found, that the dummy fans with the fixed fan blades seem to reduce the performance and quality of the measurements. For subsequent investigations it is considered to leave the cross section of the dummies empty to reduce the blockage effect, but to keep the aerodynamic surface of the DETV.

3. Conclusion and outlook

The studies presented here were intended to develop a better understanding of the Lilium jet concept, since only a few scientific data are publicly available. Therefore, a 4 step approach was defined starting with a graphical analysis of required geometric data of the vehicle concept. Despite the obvious deficiencies in accuracy of this approach, at least it provides more publicly available data than before. A NACA 4412 for the wing and canards as well as a NACA 2725 were found as good approximations. In second step handbook methods for conceptual aircraft design taken from Raymer were used to determine characteristic aerodynamic parameters like lift and drag of the approximated geometric

configuration. For the drag estimation a mismatch of the main landing gear cowling was observed resulting in an increase of drag. Neglecting this contribution a L/D ration of about 9.5 could be achieved in cruise for a C_L of 0.62, without any sucking effect of the DETV.

With this baseline a cost efficient wind tunnel model was developed using additive manufacturing methods. The modular model, which can be adapted to wing and canard setup with one measurement setup, was created using additive manufacturing methods. Deficiencies in surface quality but also accuracy in the assembly of the modules are identified as causes of inaccuracies.

The test matrix was derived from a video analysis, where the settings of the flaps and speed in different flight states were optically extracted to define 37 test cases.

The aerodynamic – propulsive coupling became visible first at the lift analysis leading to an increase in lift of up to 150% for this simplified experiment. The suction effect of the DETV is the most remarkable benefit of the entire concept over a wide range of fight states.

The analysis of the pressure distribution across the chord shows the significant beneficial effect of the tiltable DETV as part of an overall efficient design concept, where surfaces, positive lifting areas and thrust generators are integrated in a spatially highly condensed way, without losing their individual efficiency. Such compact design will at least lead to a significant reduction of the frictional drag, because the required surfaces for the airfoil and the fan cowling are minimized.

Since a precise post projection was not the goal of the studies at this stage, but first a principle understanding of the characteristics of a configuration like the Lilium Jet, this goal was achieved. At next more detailed and accurate analysis of further features will be considered, taking into account the lessons we have learned during this study. Especially the drag impact shall be more investigated. It seems, that at least the analysis of order of magnitudes should be possible following such a pragmatic and cost efficient engineering approach.

4. Copyright Statement

The authors confirm that they, and/or their company or organization, hold copyright on all of the original material included in this paper. The authors also confirm that they have obtained permission, from the copyright holder of any third party material included in this paper, to publish it as part of their paper. The authors confirm that they give permission, or have obtained permission from the copyright holder of this paper, for the publication and distribution of this paper as part of the ICAS proceedings or as individual off-prints from the proceedings.

5. References

- [1] N.N Lilium; https://lilium.com/jet; last access 02. October 2023
- [2] N.N. Lilium; https://investors.lilium.com; last access 07. May 2024
- [3] M. Niklaß, N. Dzikus, M. Swaid, J. Berling, B. Lührs, A. Lau, I. Terekhov, V. Gollnick; A Collaborative Approach for an Integrated Modeling of Urban Air Transportation Systems. Aerospace 2020, 7, 50. https://doi.org/10.3390/aerospace7050050.
- [4] N.N.; Special Condition for small-category VTOL aircraft; https://www.easa.europa.eu/sites/default/files/dfu/SC-VTOL-01.pdf; July 2nd 2019
- [5] V. Viswanathan, A.H. Epstein, et. al.; The challenges and opportunities of battery powered flight; Nature, Vol.601, pp.519-525; 2022; https://doi.org/10.1038/s41586-021-04139-1
- [6] L. Blain; Lilium's weird, energy-hungry "small fan" design could be a hidden ace; https://newatlas.com/aircraft/lilium-interview-small-fans-pros-cons/; 09. June 2021; last access: 01. October 2023
- [7] P. Nathen; Architectural performance assessment of an electric vertical take-off and landing (e-VTOL) aircraft based on a ducted vectored thrust concept, Lilium.com; 7. April 2021; https://investors.lilium.com/static-files/c355ba0f-662c-466c-aa6a-43072b3d34c3; last access: 01. October 2023
- [8] D. Wiegand; Battery Webinar The battery power behind the world's first electric VTOL Jet; November 10th, 2023, https://investors.lilium.com/events/event-details/lilium-lift-lid-battery-behind-its-revolutionary-evtol-jet-webinar-and-live-qa; last access 31st May 2024

- [9] N.N. Future Flight; Lilium Jet; https://www.futureflight.aero/aircraft-program/lilium-jet; last access: 01. October 2023
- [10] A. MacIntosh: Technology blog https://lilium.com/newsroom-detail/technology-behind-the-lilium-jet; last access 01. October 2023
- [11] V. Gollnick Assessment of the feasibility and potential of the Lilium urban air vehicle concept; contractual work for Iceberg-Research, August 2022
- [12] L. Luzi Re-Projection of a delta wing aircraft with canards; IB-M28-2022-01, Institute of Air transportation Systems, Hamburg University of Technology, Germany, November 2023, in German; not published
- [13] N.N. Introduction of a regulatory framework for the operation of drones, Notice of Proposed Amendment 2022-06, European Aviation Safety Agency (EASA), https://www.easa.europa.eu/downloads/136705/en; last access 05.08.2022
- [14] N.N: Konzeptberechnung zum Lilium-Jet; https://www.aerokurier.de/elektroflug/lilium-jet-dossier/; last access: 06.06.2022 in German
- [15] N.N: Dossier zum Lilium-Jet Hoffnungsträger oder Hochstapler; https://www.aerokurier.de/elektroflug/lilium-jet-dossier/; last access: 6.6.2022 in German
- [16] J. Lührmann, F. Danquah, A. Semke; Wind tunnel tests of a Lilium-Jet wing section; IB-M28-2023-20; Institute of Air Transportation Systems, Hamburg University of Technology; Germany; March 2023 – in German; not published
- [17] A.I. Abrego, R.W. Bulega; Performance Study of a Ducted Fan System; American Helicopter Society Aerodynamics, Acoustics, and Test and Evaluation Technical Specialists Meeting, San Francisco, CA, January 23-25, 2002. Copyright © 2002 by the American; Helicopter Society International, Inc.
- [18] H.D. Kim, A.T. Perry, P.J. Ansell; A Review of Distributed Electric Propulsion Concepts for Air Vehicle Technology; 2018 AIAA/IEEE Electric Aircraft Technologies Symposium July 9-11, 2018; Cincinnati, Ohio
- [19] A. Sgueglia, P. Schmollgruber, N. Bartoli, et. al.; Exploration and Sizing of a Large Passenger Aircraft with Distributed Ducted Electric Fans; 2018 AIAA Aerospace Sciences Meeting; 8–12 January 2018; Kissimmee, Florida; https://doi.org/10.2514/6.2018-1745
- [20] F. Danquah; Post-Projection of the Lilium-Jet considering wind tunnel tests, IB-M28-2024-5; Institute of Air Transportation Systems, Hamburg University of Technology; Germany; March 2024 in German, not published
- [21] D. P. Raymer; Aircraft Design Conceptual Approach; 6th edition, AIAA Education Series, ISBN 978-1624104909, American Institute of Aeronautics and Astronautics, 2018
- [22] M. Keho; Turboelectric Distributed Propulsion Test Bed Aircraft LEARN Phase II Final Report; Contract Number NNX14AF44A, Rolling Hills Research Corporation, 420 North Nash Street, El Segundo, CA 90245, USA, 15th Sept. 2015
- [23] N.N; Image Processing and Anaylsis in Java; https://imagej.net/ij/; last access 1st June 2024
- [24] M. Drela; "XFOIL: An Analysis and Design System for Low Reynolds Number Airfoils"; in T.J. Mueller (eds; Low Reynolds Number Aerodynamics. Lecture Notes in Engineering; Vol.54; Springer, Berlin, Germany, 1989, doi: 10.1007/978-3-642-84010-4